Multi-phase homogenization procedure for estimating the mechanical properties of shot-earth materials

M. Bacciocchi, V. Savino, L. Lanzoni, A.M. Tarantino, M. Viviani

PII: S0263-8223(22)00569-4
DOI: https://doi.org/10.1016/j.compstruct.2022.115799
Reference: COST 115799

To appear in: *Composite Structures*

Received date : 28 February 2022
Revised date : 13 May 2022
Accepted date : 17 May 2022

Please cite this article as: M. Bacciocchi, V. Savino, L. Lanzoni et al., Multi-phase homogenization procedure for estimating the mechanical properties of shot-earth materials. *Composite Structures* (2022), doi: https://doi.org/10.1016/j.compstruct.2022.115799.

Multi-phase homogenization procedure for estimating the mechanical properties of shot-earth materials

M. Bacciocchi[1,2,*], V. Savino[3], L. Lanzoni[2,4], A.M. Tarantino[2,4], M. Viviani[3]

Abstract

The paper proposes an analytical homogenization procedure to predict the overall elastic properties of shot-earth, a sustainable composite material made of excavated soil, aggregates and, if needed, a binder for stabilization. A multi-step methodology based on the Mori-Tanaka approach is used to account for the stabilized soil inclusions. This approach is proposed in order to shorten the mix-design procedures and readily provide to the structural engineers a set of mechanical properties of the shot-earth components to be used in the early design phases, when the construction field is not open yet and excavation of the site has not begun. The analytical results were successfully validated through an experimental campaign.

Key words: Shot-earth materials, Homogenization, Sustainable materials, Mori-Tanaka scheme, Experimental validation

*corresponding author

[1]DESD-Department of Economics, Science and Law, University of San Marino, San Marino

[2]CRICT-Centro di Ricerca Interdipartimentale Costruzioni e del Territorio, University of Modena and Reggio Emilia, 41125 Modena, Italy

[3]HEIG-VD/HES-SO - Haute Ecole d'Ingénierie et de Gestion du Canton de Vaud, Route de Cheseaux 1, CH-1401 Yverdon, Switzerland

[4]DIEF-Department of Engineering "Enzo Ferrari", University of Modena and Reggio Emilia, 41125 Modena, Italy

1. Introduction

Soil has been used worldwide to build and today it is still one of the most used construction materials in the world, so much that is estimated that 30% of the global population live in raw earth buildings [1]. The raw earth construction has reached a certain popularity and quality mostly in the region where a suitable soil is available [2, 3]. An appropriate soil needs little to no stabilization and provides a construction material that is durable in the surrounding environment. Traditional raw earth construction techniques [4, 5] evolved into products like the "earth concrete" [6]. Example of earth concretes developed in recent decades are the Alker, the Cast Earth [7] and the Cematerre [8]. Projected soil has been used widely for rendering and constructing walls, as well as for realizing some houses [9]. The typical limitations that hinder the adoption on a larger scale of the classical earth-based concretes include no green strength, clay-dependent mechanical performances, complexity to manage the rheology, high sensibility to water intake and difficult to manage hardening mechanisms. A recent investigation on a sustainable earth-based technology, named "shot-earth" [10], has highlighted the potential of this technology to overcome at once all the mentioned limitations. In addition, the shot-earth technology can transform the excavated soil into a new sustainable and structural building material by satisfying both engineering and environmental needs. In fact, the composition of shot-earth material includes a mixture of excavated soil and aggregates. If the soil is not suitable for the raw-earth construction, a soil stabilization is used. All compounds are mixed together and placed by shooting them at high speed, using a dry process (see Figure 1). This technology can reduce the

Figure 1: In situ spraying process of shot-earth.

exploitation and the logistic of new raw materials and promote more sustainable building processes [11, 12]. From a mechanical point of view, shot-earth has the advantage of an enhanced green strength, i.e. it is self-supporting from the moment it is placed and reach a 28-days strength of about 10 MPa, as well as an elastic modulus of about 9700 MPa. In addition, test repetitions carried out on scale specimens and cores confirmed the regularity of the mechanical characteristics. The research and the recent applications of shot-earth for constructing scale walls showed the potential of this technology as a construction material [10]. Nevertheless, each new construction field might have a different soil, that might imply a new mix-design and a new set of engineering properties. At the present time testing campaigns and new experimental techniques have supplied the data needed by designers. Even though, an easier tool for predicting which engineering properties might be reached using a specific excavated soil in a specific construction field is still needed. In fact, architect and engineers need to know the engineering properties of the materials that they might employ to construct before attempting a preliminary design. For this reason, a methodology to predict the mechanical properties of the hardened shot-earth was prepared and is presented in this paper.

The methodology is based on the knowledge of the micro, meso and macro characteristics of the basic components of shot-earth in order to obtain via few tests, on a small quantity of the soil to be excavated in field, the same results than a large testing campaign on both the components of short earth (sand, excavation earth, stabilization) and on hardened shot-earth specimens manufactured with an appropriate pump, in field. The methodology that pre-

dicts the linear elastic properties of shot-earth is based on the Mori-Tanaka approach [13], and its subsequent interpretation given by Benveniste [14]. As highlighted in the paper by Abaimov et al. [15], this method is characterized by a straightforward explicit scheme that makes it easily applicable. In the current work, this approach has been implemented adopting the multi-step procedure as proposed by Caporale et al. [16]. The methodology includes the use of the Voight and Reuss bounds and take into consideration the porosity of the medium [17]. These approaches have been also mentioned in the paper by Strazzeri et al. [18], in which the properties of cement stabilised rammed earth were discussed.

Shot-earth is a composite material made with high inclusion of excavated soil (see Figure 2). This inclusion is properly taken into account in the prediction model explained in the following. Despite the large use of earth-based

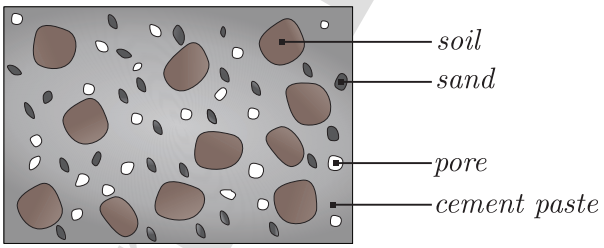

Figure 2: Shot-earth can be schematized as a porous concrete with soil inclusions.

construction materials, only few papers have been focused on the micromechanics of earth-based composites [18–20]. None of them investigated the properties on an earthen material placed by shooting like shot-earth. Therefore, all models had to be modified and driving parameters evaluated.

2. Mori-Tanaka homogenization procedure

The Mori-Tanaka method can be applied to investigate the interactions between the phases of a binary composite [21] and predicts its linear elastic mechanical characteristics. The two phases are respectively the inclusions (first constituent) and the matrix (second constituent), in which they are embedded [22]. It should be remarked that both matrix and inclusions are assumed to be isotropic. Each phase (or component) is characterized by a linear constitutive law of the type:

$$\mathbf{T}^{(i)} = \mathbb{C}^{(i)}\mathbf{E}^{(i)}, \tag{1}$$

for $i = 1, 2$, where $\mathbf{T}^{(i)}, \mathbf{E}^{(i)}$ are the stress and strain tensors, respectively. The fourth-order tensor $\mathbb{C}^{(i)}$ is the elasticity tensor. In equation (1), the index i can indicate both the matrix and the inclusions. In particular, the index $i = 1$ specifies the matrix, whereas the inclusions are denoted by $i = 2$. Relation (1) can be rewritten by using the indicial notation in order to introduce the elastic constants $[\mathbb{C}]^{(i)}_{\alpha\beta\gamma\delta}$

$$T^{(i)}_{\alpha\beta} = [\mathbb{C}]^{(i)}_{\alpha\beta\gamma\delta}\, E^{(i)}_{\gamma\delta}. \tag{2}$$

It is clear that the components of tensor $\mathbb{C}^{(i)}$ for the i-th constituent are expressed in terms of the two mechanical parameters characterizing all isotropic media: the Young's modulus $E^{(i)}$ and the Poisson's ratio $\nu^{(i)}$ [23, 24]. In the following, the components of tensor $\mathbb{C}^{(i)}$ are specified (the components that are not mentioned are null):

$$C_{1111}^{(i)} = C_{2222}^{(i)} = C_{3333}^{(i)} = \frac{E^{(i)}\left(\nu^{(i)} - 1\right)}{2\left(\nu^{(i)}\right)^2 + \nu^{(i)} - 1}, \tag{3}$$

$$C_{1122}^{(i)} = C_{1133}^{(i)} = C_{2233}^{(i)} = -\frac{E^{(i)}\nu^{(i)}}{2\left(\nu^{(i)}\right)^2 + \nu^{(i)} - 1}, \tag{4}$$

$$C_{1313}^{(i)} = C_{2323}^{(i)} = C_{1212}^{(i)} = \frac{E^{(i)}}{2\left(1 + \nu^{(i)}\right)} = G^{(i)}, \tag{5}$$

where $G^{(i)}$, for $i = 1, 2$, represent the two shear moduli, which can be expressed as a function of the other two mechanical constants $E^{(i)}$ and $\nu^{(i)}$ [25, 26].

A representative volume element is considered now to establish the average stress tensor $\bar{\mathbf{T}}$ and the average strain tensor $\bar{\mathbf{E}}$

$$\bar{\mathbf{T}} = f_1\bar{\mathbf{T}}^{(1)} + f_2\bar{\mathbf{T}}^{(2)}, \tag{6}$$

$$\bar{\mathbf{E}} = f_1\bar{\mathbf{E}}^{(1)} + f_2\bar{\mathbf{E}}^{(2)}, \tag{7}$$

in which $\bar{\mathbf{T}}^{(i)}$, $\bar{\mathbf{E}}^{(i)}$ stand for the average stress and strain tensors in the i-th constituent, which are related as follows:

$$\bar{\mathbf{T}}^{(i)} = \mathbb{C}^{(i)}\bar{\mathbf{E}}^{(i)}. \tag{8}$$

On the other hand, f_1, f_2 represent the volume fractions of the two constituents, here considered as the matrix and the inclusions. Given (8), relation (6) becomes

$$\bar{\mathbf{T}} = f_1\mathbb{C}^{(1)}\bar{\mathbf{E}}^{(1)} + f_2\mathbb{C}^{(2)}\bar{\mathbf{E}}^{(2)}. \tag{9}$$

The average strains in the i-th constituent can be written in terms of the fourth-order average strain concentration tensor $\mathbb{A}^{(i)}$

$$\bar{\mathbf{E}}^{(i)} = \mathbb{A}^{(i)}\bar{\mathbf{E}}, \tag{10}$$

for $i = 1, 2$. The introduction of this relation into (9) provides the following result:

$$\bar{\mathbf{T}} = \left(f_1 \mathbb{C}^{(1)} \mathbb{A}^{(1)} + f_2 \mathbb{C}^{(2)} \mathbb{A}^{(2)}\right) \bar{\mathbf{E}}. \tag{11}$$

The comparison with the global constitutive relation $\bar{\mathbf{T}} = \bar{\mathbb{C}}\bar{\mathbf{E}}$ leads to

$$\bar{\mathbb{C}} = f_1 \mathbb{C}^{(1)} \mathbb{A}^{(1)} + f_2 \mathbb{C}^{(2)} \mathbb{A}^{(2)}, \tag{12}$$

in which $\bar{\mathbb{C}}$ is the overall tensor of elasticity of the composite. Recalling that $\sum_{i=1}^{2} f_i \mathbb{A}^{(i)} = \mathbb{I}$, where $\mathbb{I}$ is the fourth-order identity tensor, the overall elasticity tensor assumes the following aspect:

$$\bar{\mathbb{C}} = \mathbb{C}^{(1)} + f_2 \left(\mathbb{C}^{(2)} - \mathbb{C}^{(1)}\right) \mathbb{A}^{(2)}. \tag{13}$$

Likewise, the overall compliance tensor $\bar{\mathbb{D}}$ can be defined as well

$$\bar{\mathbb{D}} = \mathbb{D}^{(1)} + f_2 \left(\mathbb{D}^{(2)} - \mathbb{D}^{(1)}\right) \mathbb{B}^{(2)}, \tag{14}$$

in which $\mathbb{D}^{(i)}$, for $i = 1, 2$, stands for the compliance tensor of the i-th constituent, whereas $\mathbb{B}^{(i)}$ represents the average stress concentration tensor that allows writing

$$\bar{\mathbf{T}}^{(i)} = \mathbb{B}^{(i)} \bar{\mathbf{T}}. \tag{15}$$

Differently than other approaches, such as the self-consistent based procedures, the Mori-Tanaka homogenization method provides an evaluation of the average fields by considering a finite subregion of the infinite composite as representative volume element [16, 22]. In particular, this method assumes that the average stress tensor of the matrix coincides with the strain tensor evaluated at infinity of the whole composite medium. As illustrated in the

paper by Klusemann et al. [22], this assumption allows to compute the strain concentration tensor $\mathbb{A}^{(2)}$ as follows:

$$\mathbb{A}^{(2)} = \mathbb{T}\left(f_1\mathbb{I} + f_2\mathbb{T}\right)^{-1}, \tag{16}$$

where the tensor $\mathbb{T}$ can be defined on the basis of the Eshelby approach for linearly elastic homogeneous bodies with ellipsoidal inclusions [27]

$$\mathbb{T} = \left[\mathbb{I} - \mathbb{S}^{(1)}\left(\mathbb{C}^{(1)}\right)^{-1}\left(\mathbb{C}^{(1)} - \mathbb{C}^{(2)}\right)\right]^{-1}. \tag{17}$$

The Eshelby tensor is denoted by $\mathbb{S}^{(1)}$ and depends on the properties of the matrix [27]. In particular, it is function only of the Poisson's ratio of the matrix $\nu^{(1)}$ and it depends on the aspect ratio of the inclusions [16, 27]. The general procedure for the computation of the Eshelby tensor in the case of linearly elastic homogeneous bodies with isotropic ellispoidal inclusions is presented in the book by Mura [28]. This procedure can be simplified assuming that the inclusions have spherical shape. In this circumstance, the components of the Eshelby tensor $[\mathbb{S}]^{(1)}_{\alpha\beta\gamma\delta}$ assume closed-form expressions. They are presented below (the components that are not specified are null), recalling its symmetric features

$$S^{(1)}_{1111} = S^{(1)}_{2222} = S^{(1)}_{3333} = \frac{7 - 5\nu^{(1)}}{15\left(1 - \nu^{(1)}\right)}, \tag{18}$$

$$S^{(1)}_{1122} = S^{(1)}_{2233} = S^{(i)}_{1133} = \frac{5\nu^{(1)} - 1}{15\left(1 - \nu^{(1)}\right)}, \tag{19}$$

$$S^{(1)}_{1313} = S^{(1)}_{1212} = S^{(1)}_{2323} = \frac{4 - 5\nu^{(1)}}{15\left(1 - \nu^{(1)}\right)}. \tag{20}$$

Further details concerning the Eshelby tensor can be found in the paper by Shi et al. [29]. On the other hand, the paper by Klusemann et al. [22], can be taken as a reference if non-elliptical inclusions have to be considered.

3. Mechanical features of shot-earth components

The mechanical characterization of the shot-earth as a multi-phase porous hardening material with excavated soil inclusions is made by means of a multi-step application of the Mori- Tanaka scheme. At each step a two-phase composite is considered. In other words, various inhomogeneities are homogenized in subsequent steps, which aim to provide the input properties for the consecutive homogenization process [15]. The following couples of constituents are analyzed:

- Step 1: Voids (denoted by v) embedded in a pure cement paste (denoted by pp), which provides the porous cement paste (denoted by p);
- Step 2: Aggregate inclusion (denoted by s) embedded in the porous cement paste, which characterizes the mortar (denoted by m);
- Step 3: Shot-earth material defined by excavated soil inclusions (denoted by e) embedded in the mortar.

It should be noted that one of the two components taken into consideration in steps 2 and 3 is the composite obtained in the previous step. The outline of the multi-step procedure is presented in Figure 3. As mentioned above, it should be considered that each constituent is assumed to be isotropic. Therefore, only two independent elastic constants are required for its complete characterization.

In the first step, the matrix (first component) is the pure cement paste. The pores (or voids), instead, represent the inclusions (second component), which are characterized by a null elastic tensor. The voids are mainly given

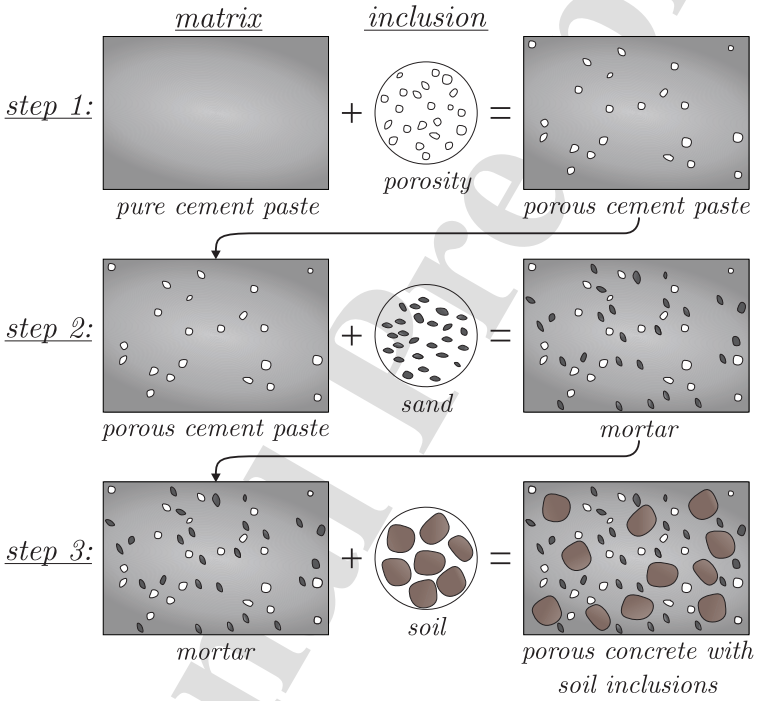

Figure 3: Chart of the three steps of the homogenization procedure.

by the presence of air in the mixture, as well as by the voids left by the evaporation of the water that is bound during the binder hydration. At this stage, the constitutive tensor $\bar{\mathbb{C}}^{(p)}$ of the porous cement paste is computed as

$$\bar{\mathbb{C}}^{(p)} = \mathbb{C}^{(pp)} - f_v \mathbb{C}^{(pp)} \mathbb{A}^{(v)}, \tag{21}$$

where f_v stands for the volume fraction of the pores and it is proportional to the water/cement ratio. As specified in [16], f_v represents the evolution law of the voids, which is given as a function of the average strain in the pure cement paste to take into account the nonlinear response of cement concrete due to the effect of the cracks. Since the current research is focused on the evaluation of the linear behavior of the material, a constant parameter is assigned to f_v, which coincides with the initial porosity of the paste. Its value is assumed less than or equal to one. Reasonably, it is included in the range $0 \div 0.5$, as can be observed in [16], and it can affect noticeably the overall properties of the final composite. Step 1 represents a preliminary homogenization scheme to characterize the porous cement paste, which is one of the three constituents of the final composite (together with aggregates and soil). Therefore, the volume fraction of voids is included only at this stage to define the effective properties of the cement and it does not appear in the relative ratio among the other constituents.

The matrix in the second step is given by the porous cement paste, whereas the inclusions are made of aggregates. This mixture represents the mortar, whose constitutive tensor $\bar{\mathbb{C}}^{(m)}$ is defined as

$$\bar{\mathbb{C}}^{(m)} = \bar{\mathbb{C}}^{(p)} + f_s \left(\mathbb{C}^{(s)} - \bar{\mathbb{C}}^{(p)} \right) \mathbb{A}^{(s)}, \tag{22}$$

where f_s is the volume fraction of the solid components of the composite at this stage.

In the third step, the role of matrix is given to the mortar, whereas the excavated soil represents the inclusions. The so-obtained shot-earth is characterized by the elasticity tensor $\bar{\mathbb{C}}^{(c)}$, which can be evaluated as follows:

$$\bar{\mathbb{C}}^{(c)} = \bar{\mathbb{C}}^{(m)} + f_e \left(\mathbb{C}^{(e)} - \bar{\mathbb{C}}^{(m)}\right) \mathbb{A}^{(e)}, \tag{23}$$

where f_e stands for the volume fraction of the soil at this step.

Finally, the constitutive law for the composite material can be expressed as

$$\bar{T}_{\alpha\beta} = \left[\bar{\mathbb{C}}\right]^{(c)}_{\alpha\beta\gamma\delta} \bar{E}_{\gamma\delta}, \tag{24}$$

with a form similar to (2). Once the elasticity tensor $\bar{\mathbb{C}}^{(c)}$ of the isotropic body is known, it is possible to compute its elastic features in terms of engineering constants, such as the Young's modulus $\bar{E}$, the shear modulus $\bar{G}$, the Poisson's ratio $\bar{\nu}$, and the bulk modulus $\bar{K}$. The following definitions can be used to this aim [30]:

$$\bar{E} = \frac{\bar{C}_{1111}^2 + \bar{C}_{1111}\bar{C}_{1122} - 2\bar{C}_{1122}^2}{\bar{C}_{1111} + \bar{C}_{1122}}, \tag{25}$$

$$\bar{G} = \frac{\bar{C}_{1111} - \bar{C}_{1122}}{2}, \tag{26}$$

$$\bar{\nu} = \frac{\bar{C}_{1122}}{\bar{C}_{1111} + \bar{C}_{1122}}, \tag{27}$$

$$\bar{K} = \frac{\bar{C}_{1111}^2 + \bar{C}_{1111}\bar{C}_{1122} - 2\bar{C}_{1122}^2}{3\bar{C}_{1111} - 3\bar{C}_{1122}}. \tag{28}$$

Since an isotropic body is characterized by two independent elastic coefficients, the quantities shown above are not all independent and relationships can be established.

4. Bounds for multi-phase composites

The definitions of the overall constitutive tensors $\bar{\mathbb{C}}$ and $\bar{\mathbb{D}}$ can be used to obtain the bounds for multi-phase composites [31, 32]. These bounds specify the maximum and minimum values of the elastic properties as a function of the constituent volume fractions. The effective properties are included within the upper and lower bounds [33], which define the range of their admissible values. A complete review of the bounding methods is presented by Watt et al. [34].

The upper bound of the elastic features of a multi-phase composite is expressed by the Voigt tensor $\bar{\mathbb{C}}_U$. It can be obtained from equation (13) by setting $\mathbb{A}^{(i)} = \mathbb{I}$, for $i = 1, 2$, as indicated by Klusemann et al. [22]. Consequently, one can assume

$$\bar{\mathbb{C}}_U = \sum_{i=1}^{2} f_i \mathbb{C}^{(i)}. \tag{29}$$

By hypothesis, the Voigt bound is also named as isostrain average, since it assumes that each constituent has the same strain, as it can be deduced from (10).

The lower bound of the elastic properties of a multi-phase composite is defined by the Reuss tensor $\bar{\mathbb{C}}_L$. With respect to the Voigt bound, the Reuss bound is known as isostress average since each constituent is characterized by the same stress. In fact, as mentioned in [22], it is assumed that $\mathbb{B}^{(i)} = \mathbb{I}$, for $i = 1, 2$. The current assumption is verified by expression (15). The Reuss tensor $\bar{\mathbb{C}}_L$ can be deduced from definition (14), recalling that the compliance

tensor is the inverse of the elasticity tensor

$$\bar{\mathbb{C}}_L = \left(\sum_{i=1}^{2} f_i \mathbb{D}^{(i)} \right)^{-1} . \tag{30}$$

The same definitions shown in Section 3 can be applied to the Voigt and Reuss tensors to evaluate the upper and lower bounds in terms of engineering constants, as shown in the book by Mavko et al. [33].

5. Experimental program

In order to predict the shot-earth mechanical properties with the proposed multi-step methodology, the elastic properties of the shot-earth components have to be known. Since the available data found in literature [10] are scarce, an experimental campaign was performed in order to provide missing data. In particular, elastic modulus and Poisson's ratio tests were carried out on the following kinds of specimens:

- Step 1: $40 \times 40 \times 160$ mm^3 prisms of porous cement paste. The cement composition used in this step was the same used to fabricate shot-earth in [10], i. e. an ordinary Portland cement;
- Step 2: Φ 160 $\times$ H320 mm cylinders of cementitious mortar composed by the same cement and aggregates used to fabricate shot-earth. The aggregate used is a standard 0/8 mm aggregate normally supplied for ordinary concrete. This aggregate is composed by local materials (Western Switzerland) namely a standard sand river 0/4 mm, with a bulk density of about 1400 kg/m^3, and a gravel 4/8 mm with a bulk density of about 1420 kg/m^3 composed by 25 % and 75 % by weight of crushed and river gravel, respectively;

- Step 3: Φ 150 × H300 mm cylinders of pressed-earth composed by the same cement, aggregates and excavated soil used to fabricate shot-earth. It should be noted that the excavated soil used in the mixture was locally supplied from a construction site. A standard consolidated triaxial compression test [35] was performed in order to measure the bulk modulus of investigated soil. The testing setup is showed in Figure 4. The triaxial compression test was conducted by applying on the soil-based specimen a differential pressure of 200 kPa for 90 minutes. Such a procedure permits to also observe the time evolution of the volumetric strain until consolidation. The bulk modulus was found to be 2.32 MPa. A particle size analysis of the excavated soil was performed, results are shown in Figure 5. According to the work by Sarro et al. [36], a soil with such a particle size distribution and a bulk modulus of about 2 MPa is expected to have a Young's modulus of about 4 MPa. In particular, the value of 4.18 MPa is reasonably taken to this aim. As far as the Poisson's ratio is concerned, its value is assumed equal to 0.14.

It should be noted that for steps 1 and 2 the fraction ratio of cement and aggregates was the same one adopted in shot-earth recipe investigated in [10]. Instead, for step 3 the amount of excavated soil inclusion was varied in order to consider the effect of its volume fraction on the elastic properties of shot-earth. In particular, three different configurations will be analyzed, and will be identified through the notation "cement/aggregate/soil", specifying the relative proportions of the solid constituents. In all steps, the specimens were prepared by homogenizing the components in a rotating pan mixer (see

Figure 4: Standard consolidated triaxial compression test performed on excavated soil specimen according to [35].

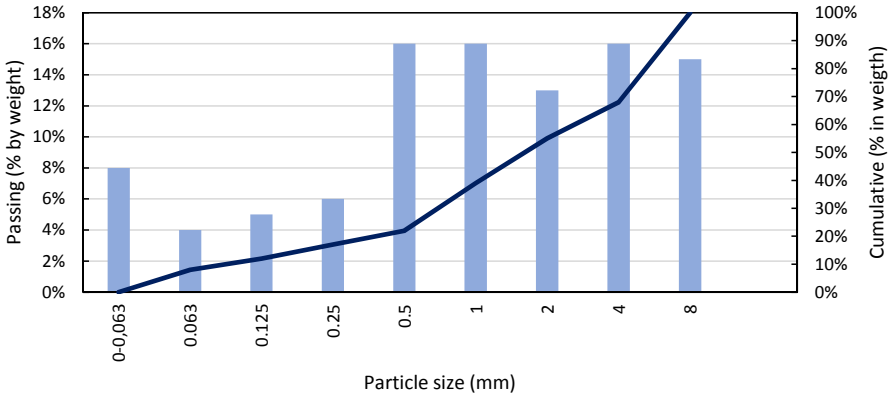

Figure 5: Particle size curve of excavated soil used to make specimens of step 3.

stage 1 in Figure 6). After five minutes of mixing, the mixture was poured in a steel formwork. In regard to specimens of step 1 (porous cement paste) and 2 (cementitious mortar), specimens of step 3 (shot-earth) were also compacted with a mechanical hydraulic press, (see Figure 6 stage 6). The compaction pressure was about 5 MPa. Then, the specimen was demolded and protected with a plastic sheet in order to slow down the water evaporation. After 28 days of curing under controlled conditions (20 ± 2°C, 60% ± 5% RH) the specimens were prepared to be mechanically tested. A Walter & Bai hydraulic press 500 kN was used to test both the Young's modulus and the Poisson's ratio of specimens of steps 1, 2 and 3. Tests were conducted according to the well established standard protocol [37, 38]. For the Poisson's ratio the test set up showed in Figure 7 was prepared to fit the geometry and size of the pressed-earth specimens. Table 1 summarizes the relevant results collected during the experimental campaign. In the same table, the results of three configurations are presented for the last step.

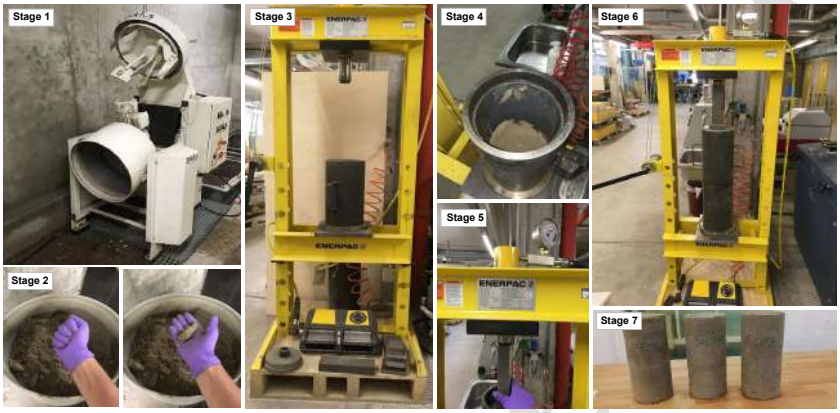

Figure 6: Stage 1: Rotation panel mixer used to make composite specimens. Stage 2: Check of workability level by a visual examination of the mixture, according to the protocol used by practitioners. Stage 3: Equipment for molding, compacting and demolding specimens of step 3. Stage 4: Inserting of the fresh mixture of step 3 within a steel formwork by setting five layers of homogeneous thick one above the other. Stage 5: Compacting each layer with a given stress level. Stage 6: Demolding specimens of step 3. Stage 7: Visual examination of specimens before curing.

Table 1: Experimental results.

Description	Constituents	Young's modulus $E^{(i)}$ (GPa)	Poisson's ratio $\nu^{(i)}$
Step 1	Porous cement past	8.38 ± 0.68	0.23 ± 0.01
Step 2	Mortar	27.97 ± 0.45	0.20 ± 0.03
	Shot-earth 2/7/2	23.02 ± 0.82	0.23 ± 0.03
Step 3	Shot-earth 2/7/7	9.71 ± 0.78	0.15 ± 0.03
	Shot-earth 2/7/10	7.25 ± 0.25	0.15 ± 0.03

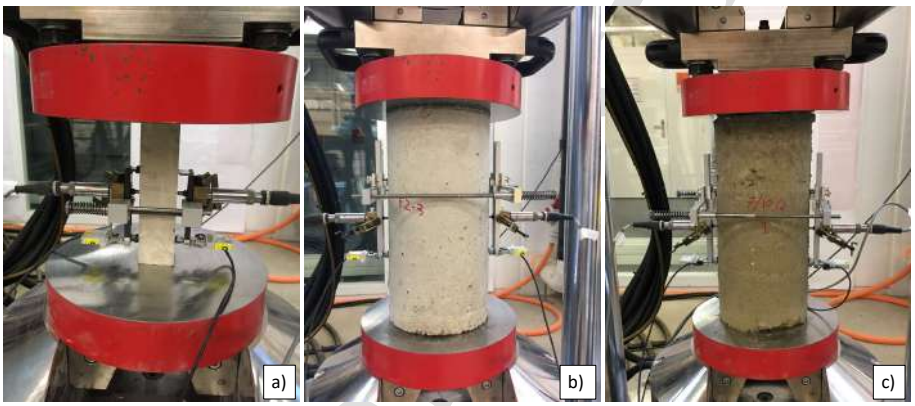

Figure 7: Experimental test performed on specimens of steps 1 (a), 2(b) and 3(c), measuring Young's modulus and Poisson's ratio according to [37] and [38] respectively.

6. Analytical results

The multi-step Mori-Tanaka approach, presented in Section 2 provides a prediction of the mechanical properties of a binary composite. Hence in step 1 the model was applied several times to a cement-voids composite with different proportion between voids and cement paste. The results presented in Table 2 are computed, as suggested by Caporale et al. [16], using a Young's modulus $E^{(pp)} = 15$ GPa and a Poisson's ratio $\nu^{(pp)} = 0.22$. Experimental results of step 1 (see Table 2 and Figure 3) match the analytical results for a porosity of $0.25 - 0.3$, a value coherent with the findings of [16]. Table 2 also highlights the importance of the quantity of voids on the mechanical characteristics.

The Mori-Tanaka model was then applied for a binary composite having as components the porous cement paste analyzed in step 1 and two groups of inhomogeneities, which are aggregates and soil. Therefore, the procedure requires two steps to provide the effective mechanical properties of the final composite. Shot-earth can be seen as a ternary mix whose volume fractions are given as: cement/aggregate/soil. A potential mix for a structural shot-earth is 2/7/7 [10]. In step 2 the mix proportion is 2/7/0 while in step 3 will be $2/7/x$, where x is a variable quantity of excavated soil assuming the values of 0, 7 and 10. In step 3, as in all steps, a binary composite is analyzed using the Mori-Tanaka approach. The composite is made by adding to the mortar calculated in step 2 (made of cement paste with voids and aggregates) the excavated soil. Thus, it is important to know the proportion between cement paste f'_p, aggregate f'_s, and excavated soil f'_e, whose values are calculated as

Table 2: Mechanical properties at step 1 of the porous cement past. Comparison with the experiment varying the volume fraction of voids f_v.

		$E^{(p)}$ (GPa)	$G^{(p)}$ (GPa)	$K^{(p)}$ (GPa)
Experiment		8.38	3.41*	5.17*
Analytical	$f_v = 0.00$	15.000	6.148	8.929
	$f_v = 0.05$	13.570	5.567	8.044
	$f_v = 0.10$	12.270	5.038	7.246
	$f_v = 0.15$	11.083	4.554	6.523
	$f_v = 0.20$	9.995	4.110	5.865
	$f_v = 0.25$	8.995	3.701	5.263
	$f_v = 0.30$	8.072	3.323	4.711
	$f_v = 0.35$	7.217	2.973	4.202

* $G^{(p)}$, $K^{(p)}$ are evaluated analytically by using the Poisson's ratio $\nu^{(p)} = 0.23$ obtained experimentally.

follows:

$$f'_p = \frac{2}{7+2+x}, \quad f'_s = \frac{7}{7+2+x}, \quad f'_e = \frac{x}{7+2+x}. \tag{31}$$

These values represent the relative volume fractions of the constituents in the final composite. It can be noted that the proportions depend on the quantity of excavated soil (denoted by x) inserted in the mixture.

In order to apply the proposed multi-step methodology, it is necessary to evaluate the relative volume fractions of the inclusions at each step, taking into account only the involved constituents in the scheme. In particular, as specified in the previous Sections, f_s and f_e denote the relative volume fractions of the solids components at step 2 and step 3, which are the two stages that provide the effective elastic properties of the shot-earth. In this circumstance, a relation between f_s, f_e, which are needed in the two following steps, and the relative volume fractions of the constituents in the final composite f'_p, f'_s, f'_e can be carried out. As shown in the paper by Abaimov et al. [15], one gets the following expressions:

$$f_s = \frac{f'_s}{1-f'_e}, \quad f_e = f'_e, \tag{32}$$

which also prove the results shown in [16].

In step 2 a Young's modulus $E^{(s)} = 45$ GPa and Poisson's ratio $\nu^{(s)} = 0.23$ were employed to compute the mechanical properties of the binary composite made combining the porous cement paste and the aggregate. These values for $E^{(s)}$ and $\nu^{(s)}$ are coherent with the literature [39–41]. In step 3 the composite obtained in step 2 was combined with the excavated soil to predict the properties of a shot-earth characterized by volume proportions $2/7/x$. The calculations were made using, for the soil fraction, the Young's modulus

and the Poisson's ratio determined experimentally. Step 3 provided three sets of results for three different shot-earth mixtures characterized by volume proportions of $2/7/x$ where x assumed the values 0, 2, 7 and 10, respectively (for $x = 0$, step 2 was achieved). During the experimental campaign shot-earth specimens were produced using the same three mixes. Test results are compared with the multi-step Mori-Tanaka predictions obtained modeling the inclusions as spherical. In Figures 8, 9 and 10 the experimental values and model predictions are presented. Figures also show the variation of the Young's modulus $\bar{E}$, shear modulus $\bar{G}$ and bulk modulus $\bar{K}$ as a function of the volume fraction f_e and as a function of the volume fraction of the porosity f_v. The upper and lower bounds are depicted in all graphs. Reuss (lower) bound is low since this specific soil is a weak construction material and therefore its mechanical characteristics have a much lower value than the mortar.

It can be observed that the analytical results predicted by the Mori-Tanaka approach are close to the experimental values and therefore the model can predict the elastic properties of shot-earth. Consequently, once the properties of shot-earth components are known, especially those of soil inclusions, it can be possible identify which kind of civil engineering applications might be made with a specific excavation soil. It should be also highlighted that the choice of the aggregate's properties made in this study is correct since the prediction of the mechanical properties of the composite for $f_e = 0$ matches the experimental values. It should be recalled that $f_e = 0$ defines the second step of the procedure as defined in the previous Sections. Figures 8, 9 and 10 show also, as expected, the importance of the porosity taken into ac-

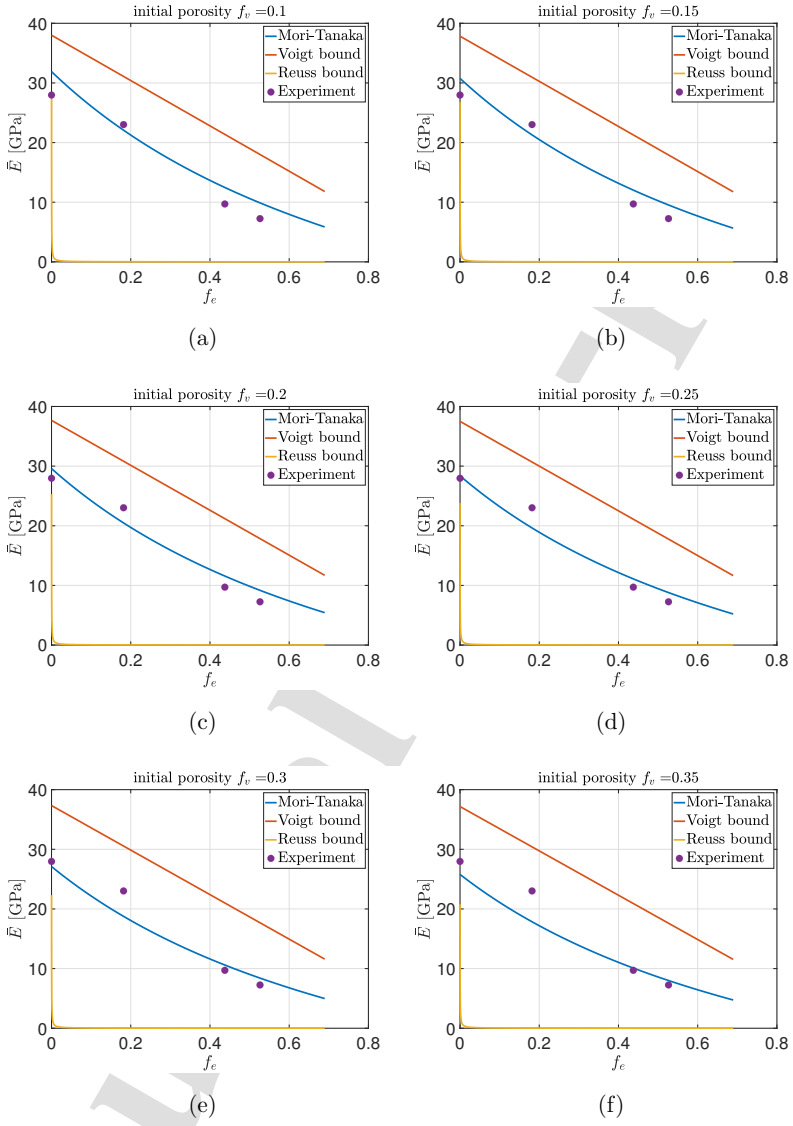

Figure 8: Evaluation of the Young's modulus $\bar{E}$ of the composite as a function of the volume fraction f_e, for different values of the porosity f_v. The inclusions are modeled as spherical.

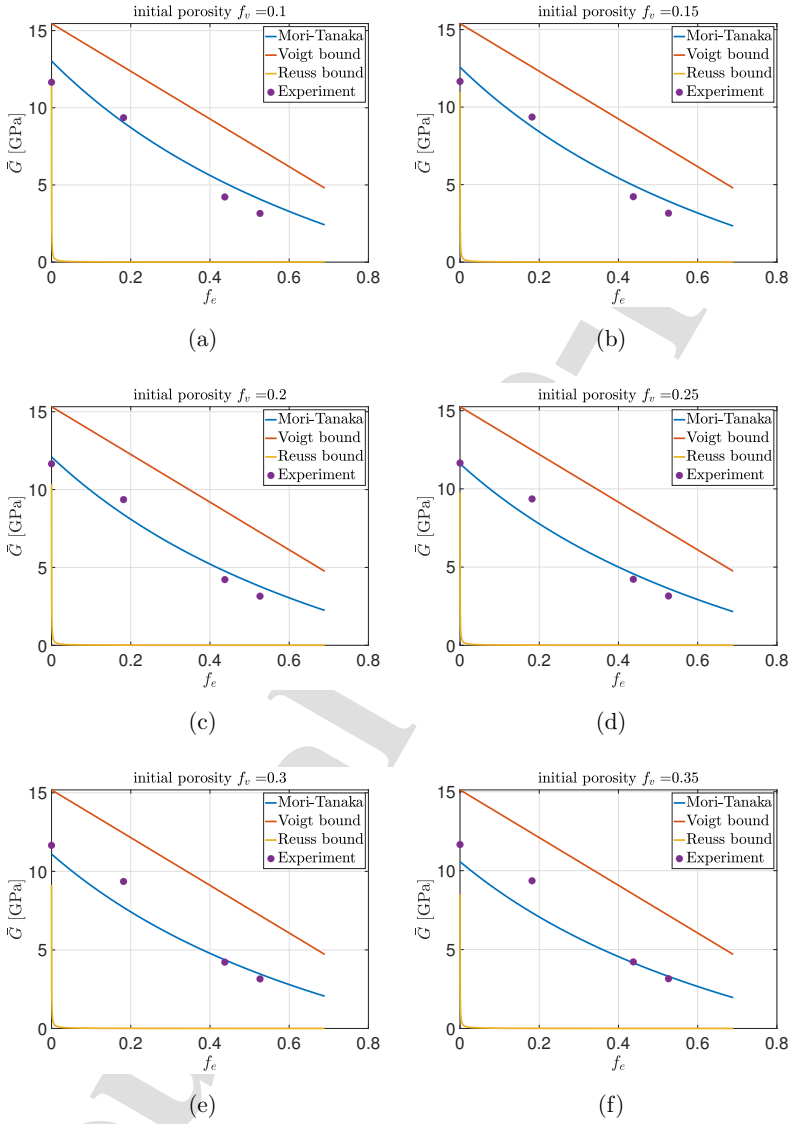

Figure 9: Evaluation of the shear modulus $\bar{G}$ of the composite as a function of the volume fraction f_e, for different values of the porosity f_v. The inclusions are modeled as spherical.

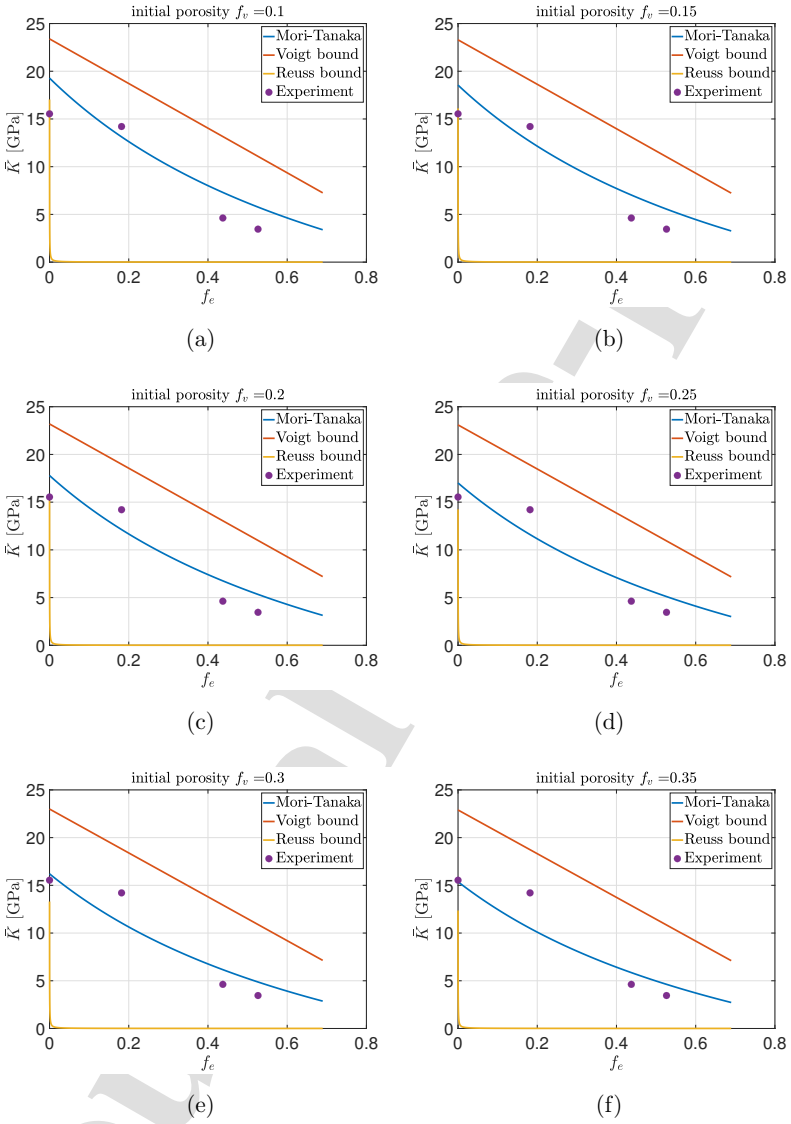

Figure 10: Evaluation of the bulk modulus $\bar{K}$ of the composite as a function of the volume fraction f_e, for different values of the porosity f_v. The inclusions are modeled as spherical.

count through f_v: an increasing value of the porosity affects the mechanical properties. Furthermore, as expected, for $f_v = 0.25 - 0.3$ the best agreement between the analytical results and the experimental properties is obtained. A final observation can be introduced, following the conclusions introduced in the papers by Naili et al. [42] and Koutsawa et al. [43], to discuss the choice of the order of the homogenization steps. In the present paper, the order proposed by Caporale et al. [16] has been followed, replacing the gravel at stage 3 with the excavated soil. The validity of this strategy has been confirmed by the good agreement between the experimental and analytical results. In addition, the predictions of the engineering constants lie between the Voigt and Reuss bounds. The same level of accuracy could not be reached, for instance, by switching the order of soil and sand in the homogenization process, if compared to the experimental values, and the curves of the analytical results would tend to approach the lower bound. This confirms the importance of the order of the constituents [42].

7. Final remarks

In [10] a new sustainable material called shot-earth is presented. Shot-earth is made of excavated soil, aggregate and, if needed, a binder for stabilization. Excavation soil can have much different characteristics according to the location of the construction site. Consequently, a practical method to predict which civil engineering applications are possible with a specific soil is needed, by minimizing the costs of both field trial and the equipment requested. The proposed methodology can be applied *a priori*, before the realization of the construction in a specified location. Its aim, in fact, is the

preliminary evaluation of the mechanical properties of the shot-earth material that could be obtained by using the soil which is excavated from that particular site. In this paper, the shot-earth is modeled as a multi-phase material and an analytical procedure based on a multi-step application of the Mori-Tanaka approach has been used to predict its mechanical properties. The model is simple to use and can predict the elastic modulus, shear modulus and bulk modulus of shot earth as a function of the volume fraction of shot-earth components and of the porosity. The predictions of the model were validated by means of a wide experimental campaign.

Declaration of Competing Interest

The authors declare that they have no known competing financial interests or personal relationships that could have appeared to influence the work reported in this paper.

Acknowledgments

Financial support from the HES-SO in the framework of the Project NEB NextEarthBuilding is gratefully acknowledged. Financial support from the Italian Ministry of University and Research (MUR) in the framework of the Project FISR 2019: "Eco_Earth" (code 00245) and in the framework of the Project PRIN 2017 "Modelling of constitutive laws for traditional and innovative building materials" (code 2017HFPKZY) are gratefully acknowledged.

Data availability

The raw/processed data required to reproduce these findings cannot be shared at this time as the data also forms part of an ongoing study.

References

[1] M. Schweiker, E. Endres, J. Gosslar, N. Hack, L. Hildebrand, M. Creutz, A. Klinge, H. Kloft, U. Knaack, J. Mehnert, et al., Ten questions concerning the potential of digital production and new technologies for contemporary earthen constructions, Building and Environment 206 (2021) 108240.

[2] H. Houben, H. Guillaud, Traité de construction en terre, Woodhead Pub Ltd, 2014.

[3] F. Parisi, D. Asprone, L. Fenu, A. Prota, Experimental characterization of italian composite adobe bricks reinforced with straw fibers, Composite Structures 122 (2015) 300–307.

[4] H. Houben, H. Guillaud, Earth construction: a comprehensive guide, www.greenhomebuilding.com.

[5] G. Lan, Y. Wang, G. Zeng, J. Zhang, Compressive strength of earth block masonry: Estimation based on neural networks and adaptive network-based fuzzy inference system, Composite Structures 235 (2020) 111731.

[6] H. Van Damme, H. Houben, Earth concrete. stabilization revisited, Cement and Concrete Research 114 (2017) 90–102.

[7] Cast earth, www.greenhomebuilding.com.

[8] J. M. Kanema, The influence of soil content on the mechanical properties, drying shrinkage and autogenous shrinkage of earth concrete, Journal of Building Engineering 13 (2017) 68–76.

[9] M. R. Hall, R. Lindsay, M. Krayenhoff, Modern Earth Buildings, Woodhead Pub Ltd, 2012.

[10] A. Curto, L. Lanzoni, A. M. Tarantino, M. Viviani, Shot-earth for sustainable constructions, Construction and Building Materials 239 (2020) 117775.

[11] H. Porter, J. Blake, N. K. Dhami, A. Mukherjee, Rammed earth blocks with improved multifunctional performance, Cement and Concrete Composites 92 (2018) 36–46.

[12] M. Beccali, V. Strazzeri, M. Germanà, V. Melluso, A. Galatioto, Vernacular and bioclimatic architecture and indoor thermal comfort implications in hot-humid climates: An overview, Renewable and Sustainable Energy Reviews 82 (2018) 1726–1736.

[13] T. Mori, K. Tanaka, Average stress in matrix and average elastic energy of materials with misfitting inclusions, Acta metallurgica 21 (5) (1973) 571–574.

[14] Y. Benveniste, A new approach to the application of mori-tanaka's theory in composite materials, Mechanics of materials 6 (2) (1987) 147–157.

[15] S. G. Abaimov, A. Trofimov, I. V. Sergeichev, I. S. Akhatov, Multi-step homogenization in the mori-tanaka-benveniste theory, Composite structures 223 (2019) 110801.

[16] A. Caporale, L. Feo, R. Luciano, Damage mechanics of cement concrete modeled as a four-phase composite, Composites Part B: Engineering 65 (2014) 124–130.

[17] M. Kamiński, A. Pawlak, Various approaches in probabilistic homogenization of the cfrp composites, Composite Structures 133 (2015) 425–437.

[18] V. Strazzeri, A. Karrech, M. Elchalakani, Micromechanics modelling of cement stabilised rammed earth, Mechanics of Materials 148 (2020) 103540.

[19] Q. Piattoni, E. Quagliarini, S. Lenci, Experimental analysis and modelling of the mechanical behaviour of earthen bricks, Construction and Building Materials 25 (4) (2011) 2067–2075.

[20] A. Karrech, V. Strazzeri, M. Elchalakani, Improved thermal insulance of cement stabilised rammed earth embedding lightweight aggregates, Construction and Building Materials 268 (2021) 121075.

[21] J. Aboudi, Mechanics of composite materials: a unified micromechanical approach, Elsevier, 2013.

[22] B. Klusemann, H. Böhm, B. Svendsen, Homogenization methods for multi-phase elastic composites with non-elliptical reinforcements: Com-

parisons and benchmarks, European Journal of Mechanics-A/Solids 34 (2012) 21–37.

[23] M. Pelliciari, A. M. Tarantino, Equilibrium paths for von mises trusses in finite elasticity, Journal of Elasticity 138 (2) (2020) 145–168.

[24] M. Pelliciari, A. M. Tarantino, Equilibrium paths of a three-bar truss in finite elasticity with an application to graphene, Mathematics and Mechanics of Solids 25 (3) (2020) 705–726.

[25] F. O. Falope, M. Pelliciari, L. Lanzoni, A. M. Tarantino, Snap-through and eulerian buckling of the bi-stable von mises truss in nonlinear elasticity: A theoretical, numerical and experimental investigation, International Journal of Non-Linear Mechanics 134 (2021) 103739.

[26] M. Pelliciari, D. P. Pasca, A. Aloisio, A. M. Tarantino, Size effect in single layer graphene sheets and transition from molecular mechanics to continuum theory, International Journal of Mechanical Sciences 214 (2022) 106895.

[27] J. D. Eshelby, The determination of the elastic field of an ellipsoidal inclusion, and related problems, Proceedings of the royal society of London. Series A. Mathematical and physical sciences 241 (1226) (1957) 376–396.

[28] T. Mura, Micromechanics of defects in solids, Springer Science & Business Media, 2013.

[29] D.-L. Shi, X.-Q. Feng, Y. Y. Huang, K.-C. Hwang, H. Gao, The effect of nanotube waviness and agglomeration on the elastic property of carbon

nanotube-reinforced composites, Journal of Engineering Materials and Technology 126 (3) (2004) 250–257.

[30] A. Kalamkarov, H. Liu, A new model for the multiphase fiber–matrix composite materials, Composites Part B: Engineering 29 (5) (1998) 643–653.

[31] L. Liu, Hashin-shtrikman bounds for multiphase composites and their attainability, Proceedings of the Royal Society A: Mathematical, Physical and Engineering Science 466 (2010) 3693–3713.

[32] S. Brisard, L. Dormieux, D. Kondo, Hashin–shtrikman bounds on the bulk modulus of a nanocomposite with spherical inclusions and interface effects, Computational Materials Science 48 (3) (2010) 589–596.

[33] G. Mavko, T. Mukerji, J. Dvorkin, The rock physics handbook, Cambridge University Press, 2020.

[34] J. P. Watt, G. F. Davies, R. J. O'Connell, The elastic properties of composite materials, Reviews of Geophysics 14 (4) (1976) 541–563.

[35] Geotechnical investigation and testing — laboratory testing of soil — part 9: Consolidated triaxial compression tests on water saturated soils, ISO 17892 9 (2018).

[36] W. Sarro, G. Ferreira, Soil elastic modulus determined by ultrasound tests, Soils and Rocks 42 (2019) 117–126.

[37] Products and systems for the protection and repair of concrete struc-

tures - determination of modulus of elasticity in compression, EN 13412 (2006).

[38] Standard test method for static modulus of elasticity and poisson's ratio of concrete in compression, C469/C469M -14 (2014).

[39] Á. Kézdi, L. Rétháti, Handbook of soil mechanics, Vol. 1, Elsevier Amsterdam, 1974.

[40] M. Prat, P. Bisch, A. Millard, P. Mestat, G. Pijaudier-Calot, et al., La modélisation des ouvrages, 1995.

[41] R. Obrzud, The hardening soil model: A practical guidebook, Zace Services, 2010.

[42] C. Naili, I. Doghri, J. Demey, Porous materials reinforced with short fibers: Unbiased full-field assessment of several homogenization strategies in elasticity, Mechanics of Advanced Materials and Structures (2021) 1–16.

[43] Y. Koutsawa, G. Rauchs, D. Fiorelli, A. Makradi, S. Belouettar, A multi-scale model for the effective electro-mechanical properties of short fiber reinforced additively manufactured ceramic matrix composites containing carbon nanotubes, Composites Part C: Open Access 7 (2022) 100234.

Author statement

M. Bacciocchi: Conceptualization, Methodology, Software, Validation, Formal analysis, Investigation, Resources, Data Curation, Writing - Original Draft, Writing - Review & Editing, Visualization, Supervision, Project administration.

V. Savino: Conceptualization, Methodology, Software, Validation, Formal analysis, Investigation, Resources, Data Curation, Writing - Original Draft, Writing - Review & Editing, Visualization, Supervision, Project administration.

L. Lanzoni: Conceptualization, Methodology, Software, Validation, Formal analysis, Investigation, Resources, Data Curation, Writing - Original Draft, Writing - Review & Editing, Visualization, Supervision, Project administration.

A.M. Tarantino: Conceptualization, Methodology, Software, Validation, Formal analysis, Investigation, Resources, Data Curation, Writing - Original Draft, Writing - Review & Editing, Visualization, Supervision, Project administration.

M. Viviani: Conceptualization, Methodology, Software, Validation, Formal analysis, Investigation, Resources, Data Curation, Writing - Original Draft, Writing - Review & Editing, Visualization, Supervision, Project administration.

Declaration of interests

☒ The authors declare that they have no known competing financial interests or personal relationships that could have appeared to influence the work reported in this paper.

☐ The authors declare the following financial interests/personal relationships which may be considered as potential competing interests: